Spatial filtering efficiency of monostatic biaxial lidar: analysis and applications

Ravil R. Agishev and Adolfo Comeron

Results of lidar modeling based on spatial-angular filtering efficiency criteria are presented. Their analysis shows that the low spatial-angular filtering efficiency of traditional visible and near-infrared systems is an important cause of low signal/background-radiation ratio (SBR) at the photodetector input. The low SBR may be responsible for considerable measurement errors and ensuing the low accuracy of the retrieval of atmospheric optical parameters. As shown, the most effective protection against sky background radiation for groundbased biaxial lidars is the modifying of their angular field according to a spatial-angular filtering efficiency criterion. Some effective approaches to achieve a high filtering efficiency for the receiving system optimization are discussed. © 2002 Optical Society of America

OCIS codes: 010.3640, 080.2720, 330.6110, 280.3640.

1. Introduction

A customarily stated rule of thumb in the design of visible and near-infrared lidar receiving optics is that the field of view should match the atmosphere illuminated cone.[1–4] This would ensure that only the background radiation coming from the same directions as the useful signal would be obtained. However, in general this is not a practical rule, because it ignores the displacement of the scattering volume image in the receiver as a function of the range occurring in a monostatic biaxial lidar system (i.e., a lidar with a small initial base L between the optical axes of the receiver and the transmitter) and defocusing effects due to the finite size of the receiving aperture, especially important for scattering volumes at short ranges. In practice usually a larger reception field of view is needed to ensure catching all of the useful signals, which entails an increase of the background radiation reaching the photodetector.

By assessing the effects of image displacement, one can tailor the lidar-receiver field of view in a practical way so as to reject (spatially filter out) to the maximum possible extent the background radiation while preserving the useful returned signal. For example, to reduce a power of background radiation entering to the receiving system, one can form the angular field of a monostatic biaxial lidar by means of a round field diaphragm, the hole size of which is chosen from the condition of undistorted passing of signals that come from the trace in the range interval ($R_{\min}$, $R_{\max}$).[4,5] Although herewith a coming background light is subjected to some restriction, an efficiency of background selection turns out not to be high.

A known way of tracking the scattering volume and its spatial displacements on the image plane seeks to compensate the R^2 range factor appearing in the denominator of the lidar equation.[6–8] The essence of the method consists of a vignetting of the signals coming from the near layers of the investigated medium, in inverse proportion to the square of current range, stopping this vignetting for the signals backscattered from the layer at $R_{\max}$. As a result one can reduce considerably the dynamic range of the received echo signals to prevent information losses when relatively narrow-range photoreceiving devices are used. Technical realizations of the R^2-compensating optical elements doing such a vignetting can differ, but very often they have the problem of being subject to responsivity inhomogeneities over the photodetector area, which may lead to significant errors in the range factor compensation and consequently a degradation of the measurement accuracy.[3] From the standpoint of stability against background, many of these optical compensators are extremely

The authors are with the Department de Teoria del Senyal i Comunicacions, Universitat Politecnica de Catalunya, Jordi Girona, 1-3, D4-100, Barcelona 08034, Spain. R. R. Agishev (agishev@tsc.upc.es) is currently on leave from Kazan State Technical University, 10, K. Marx Str., Kazan, Tatarstan 420111, Russia.

Received 27 February 2002; revised manuscript received 3 September 2002.
0003-6935/02/367516-06$15.00/0

inefficient when working on small ranges, close to the minimum range of sounding.

The following sections present the fundamentals and the practical implementation of techniques that allow us to improve the spatial-filtering efficiency of monostatic biaxial lidar systems.

2. Criterion of Spatial-Angular Filtering Efficiency for Biaxial Lidar

For common monostatic lidars the assumption that the fields of view for signal and background radiation are the same is not sufficiently correct. During biaxial lidar operation the farther the pulse scattering volume is from the apparatus, the less the distance between the volume image and the receiving optics focal plane is. Therefore along the sounding process the shape and the area of the scattering volume image are changed. The deeper the sounding range is, the more considerable these changes are. As a rule, for such systems the instantaneous signal field of view is considerably less than the field of view for background radiation. That is why the real signal–background ratio is strongly different from the one estimated by the traditional approach.

Let us introduce a figure of merit J as a spatial-angular filtering efficiency criterion of the system

$$J = \Omega_s/\Omega_0, \tag{1}$$

where Ω_s is the signal field of view and Ω_0 is the receiver field of view.

Practically, the angular field Ω_0 of the receiver is the background radiation angular field $\Omega_b(\Omega_0 = \Omega_b)$ for systems in which the background fills up all the angular field of the receiving optics. This condition will be assumed in the following discussion.

3. Instantaneous Angular Field for Return Signal

The receiving objective of the lidar gathers the radiation scattered by the atmosphere and focuses it on the image plane. According to the optical systems theory the image M' of a point M at a distance R of an unaberrated image-forming optical system, is away from the focal plane a distance z and is displaced from the optical axis a distance x:

$$z(R) = f^2/(R - f); \qquad x(R) = Lf/(R - f), \tag{2}$$

where f is the system focal length.

As it is clear from Fig. 1, for the simplified model of the transmitted beam with initial diameter d_0 and beam divergence θ_0, the beam diameter at distance R and with point M as a center is $d(R) = d_0 + R\theta_0$; then the image diameter with center in point M' is equal to

$$W(R) = (d_0 + \theta_0 R) f/(R - f). \tag{3}$$

The centers of the images of the scattering volumes lay on a straight line forming an angle $\gamma = \mathrm{arctg}(f/L)$ with the focal plane of the receiving optics. Then the instantaneous angular field of the lidar system for signal is:

$$\Omega_s(R) = S(R)/[z(R) + f]^2,$$

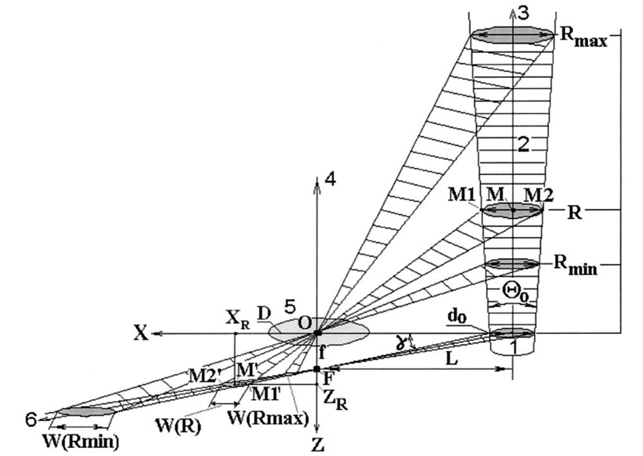

Fig. 1. Optical scheme to explain the shift of the scattering-volume image in monostatic biaxial lidar. 1, beam output aperture; 2, probing beam; 3, optical axis of transmitter; 4, optical axis of receiving system; 5, receiving lens; 6, optical axis of monitoring trace image.

where $S(R)$ is the area of the spot with diameter $W(R)$.

When a path range from $R_{\min}$ to $R_{\max}$ is sounded the image of the scattering volume shifts from a circle with center coordinates $[x(R_{\min}), z(R_{\min})]$ and diameter $W(R_{\min})$ to a circle with center coordinates $[x(R_{\max}), z(R_{\max})]$ and diameter $W(R_{\max})$.[3] The angular field of view changes accordingly.

4. Spatial-Angular Filtering Efficiency of Typical Lidar Systems

In case of typical monostatic systems, the field of view of receiving optics is determined by a field diaphragm placed in the objective image plane. At the chosen minimal sounding range $R_{\min}$, the diameter of the image spot is

$$W(R_{\min}) = (d_0/R_{\min} + \theta_0) f.$$

A. Round Diaphragm

Although for scattering signals coming from far atmosphere slices the image size will be considerably less than $W(R_{\min})$, one chooses the field diaphragm diameter according to $R_{\min}$, taking into account the spot shift span from the optical axis (Fig. 2):

$$d_{D1} = [x(R_{\min}) - x(R_{\max})] + [W(R_{\min}) + W(R_{\max})]/2,$$

where $x(R)$ is given by the second of expressions (2), and the value of $z(R)$ is small.

But choosing the stop diameter in that way leads to a large angular field for the background radiation, and to a value $J \ll 1$ that may impair the measurement accuracy. Indeed, one can obtain, taking into account Eqs. (2) and (3), and considering $R_{\max} \gg R_{\min}$ and $R_{\min} \gg f$,

$$d_{D1} = [(d_0/2 + L)/R_{\min} + \theta_0] f.$$

Assuming that the signal and background fields of view are given respectively by $\Omega_s = S_i(R)/f^2$ and $\Omega_o =$

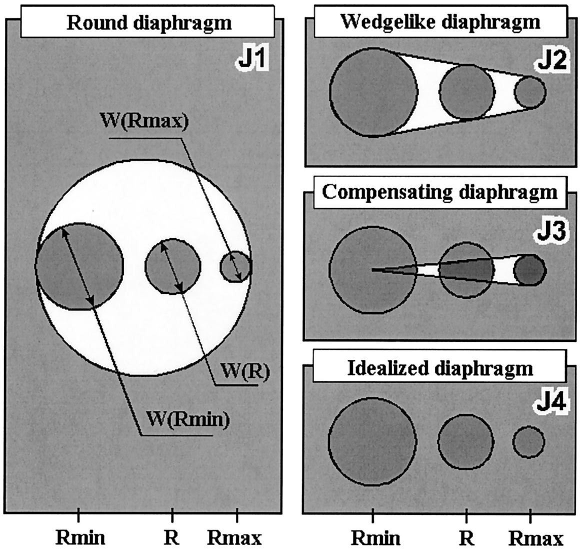

Fig. 2. Relations between the cross section of signals from ranges $R_{\min}$, R, and $R_{\max}$ and the background radiation cross section in the sounded-path image locus for different field-of-view diaphragms.

S_o/f^2 (where S_i and S_o are respectively the areas of the image of the scattering volume and the stop), the spatial-angular efficiency (1) of the optical system with a field stop diameter d_{D1} is

$$J_1 = \frac{(d_0/R + \Theta_0)^2}{\left(\frac{d_0/2 + L}{R_{\min}} + \Theta_0\right)^2}. \tag{4}$$

As an example let us take typical values for the parameters of a lidar optical system as follows: $\Theta_0 = 10^{-3}$ rad, $f = 1$ m, $d_0 = 0.02$ m, and the distance between the transmitted-beam axis and the receiving-system optical axis (lidar base) $L = 0.5$ m. The function $J_1(R/R_{\min})$ is represented in Fig. 3.

As shown, the spatial filtering efficiency of this optical system is low. At the same time, if there are tolerances in the mutual orientation of the transmitting and receiving optics axes, we must accept a larger diaphragm diameter.

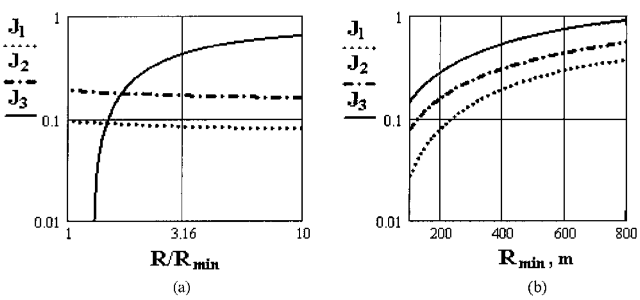

Fig. 3. (a) Spatial-angular efficiency versus normalized distance $R/R_{\min}$ function for optical systems with round (J_1), wedgelike (J_2), and compensating (J_3) diaphragms at $R_{\min} = 0.2$ km; (b) Spatial-angular efficiency as minimal sounding range $R_{\min}$ [m] function for optical systems with round, wedgelike and compensating diaphragms at $R \gg R_{\min}$. Curves are computed for $\theta_0 = 1$ mrad, $f = 1$ m, $L = 0.5$ m.

B. Wedgelike Diaphragm

The lidar field stop can be chosen in a more suitable way. According to the form of the scattering-volume image trace, given by Eqs. (2) and (3) and shown in Fig. 1, if the mutual orientation of the transmitter and receiver optics is fixed, a diaphragm shaped as the "image trace" would accept the lidar backscattered radiation from the $R_{\min}$ to $R_{\max}$ range[3] while limiting the background radiation reaching the detector. This trace looks like a wedge with round ends (Fig. 2).

As it has been shown, for a monostatic biaxial lidar the size of the scattering volume image decreases as the light pulse propagates away from the transmitter [Eq. (3)], as does the displacement from the focal plane and from the receiving-system optical axis. Likewise, as discussed in Section 3, the locus of image centers lies on a line forming an angle $\gamma = \operatorname{arctg} f/L$ with the focal plane (Fig. 1). That means the stop previously discussed should form the angle γ with respect to the focal plane.

As the coordinates (x_1, z_1) of point M_1 and (x_2, z_2) of point M_2 are

$$[Lf/(R_{\max} - f), f^2/(R_{\max} - f)]$$

and

$$[Lf/(R_{\min} - f), f^2/(R_{\min} - f)],$$

the projection of the wedge-shaped diaphragm area on the focal plane can be calculated approximately as

$$S_{D2p} = \frac{W(R_{\min}) + W(R_{\max})}{2}(x_2 - x_1) + \pi\frac{W^2(R_{\min}) + W^2(R_{\max})}{8}.$$

And taking into account Eq. (3), it can be shown that for $R_{\max} \gg R_{\min}$, $R_{\min} \gg f$, and $\theta_0 \gg d_0/R_{\min}$,

$$S_{D2p} = \frac{f^2}{2}\left[\left(\frac{d_0}{R_{\min}} + 2\theta_0\right)\frac{L}{R_{\min}} + \frac{\pi}{2}\left(\frac{d_0}{R_{\min}} + \theta_0\right)\theta_0\right].$$

Then the spatial-angular filtering efficiency of such system is

$$J_2 = \frac{S_i}{S_{D2p}} = \frac{\frac{\pi}{2}\left(1 + \frac{d_0}{R\theta_0}\right)^2}{\left(2 + \frac{d_0}{R_{\min}\theta_0}\right)\frac{L}{R_{\min}\theta_0} + \frac{\pi}{2}\left(1 + \frac{d_0}{R_{\min}\theta_0}\right)}. \tag{5}$$

The result is plotted in Fig. 3 for the typical system parameters used in Subsection 4.A. For such a system an increase of filtering efficiency J_2 is observed in comparison with J_1, though still $J_2 \ll 1$.

C. R^2-Factor Compensating Diaphragm

To a range of cases nonround diaphragms of compensating type can be applied.[4–7] These cases are intended for the reduction of the dynamic range of the received lidar signals (in most cases by range square compensation). Let us evaluate the receiving-system efficiency in background-radiation protection, when the compensating diaphragm vignettes the radiation flow that comes from short distances, providing a range square (R^2) compensation, and does not vignette signals coming from distant layers. Considering S_{D3} to be the diaphragm area, the spatial-angular filtering efficiency of such a system can be written as

$$J_3 = S_i K_v / S_{D3},$$

where $K_v = S_x/S_i$ is the received flow vignetting coefficient, S_x is the area of intersection of the image spot and the compensating diaphragm, and S_i is the image-spot area. It is clear that $J_3 = S_x/S_{D3}$. A shape of compensating diaphragm is shown in Fig. 3.

It can be shown that the following relations hold[3]:

$$S_x = [1 - x(R)/a] W(R) W(R_{\min}),$$
$$S_{D3} = W(R_{\min})[a/2 + \pi W(R_{\min})/8],$$

where $a = f(L/R_{\min} - L/R_{\max} - \theta_0/2)$, and $x(R)$ is determined from Eq. (2).

Using Eq. (3), and assuming again $R_{\max} \gg R_{\min}$, $R_{\min} \gg f$, and for $a_\infty = f(L/R_{\min} - \theta_0/2)$ the efficiency J_3 can be written as

$$J_3 = \frac{8[1 - x(R)/a_\infty]\Theta_0}{\pi\Theta_0 + 4a_\infty}. \qquad (6)$$

The analysis shows that the background filtering efficiency J_3 is high for long ranges, but at short sounding distances the vignetting of lidar signal significantly worsens the signal–background-radiation ratio (see Fig. 3).

Thus we conclude that common systems may have a low spatial-angular filtering efficiency J against background radiation, and it can be much less than 1. The spatial-angular-background filtering efficiency is sensitive to the absolute value of $R_{\min}$ and can drop below of the 0.1 level, as shown in Fig. 3. Low values of merit of the J figure lead to low signal–background ratio at the photodetector input, which may result in poor measurement accuracy.

5. Optimal Field-of-View of Biaxial Lidar

As one can see from the section 4, common systems may have a low spatial-angular filtering efficiency J against background radiation, and it can be much less than 1. That leads to low signal–background ratio at the photodetector input, and low measurement accuracy may take place.

If the lidar receiver follows the scattering impulse volume on current distance R along a sounded trace (Fig. 2, J4), it is possible to minimize the receiving optical system's angular field for background radiation. For unaberrated optics the optimal angular field to receive all of the echo signal can be determined from the following:

$$\Theta_{\text{opt}}(R) R = \Theta_0 R + d_0,$$

where the right part of the expression corresponds to the probing beam diameter on range R. Following the scattering impulse volume at short distances (about $R_{\min}$) is the most important aspect of the method from the standpoint of protection against background radiation. It allows minimizing the measuring error conditioned by background radiation. At long distances a relation $\theta_{\text{opt}} = \theta_0$ will be correct.

As a rule for common lidar, the use of the operation range ($R_{\min}$, $R_{\max}$) and with a circular field stop placed in the focal plane, the first approximation of the receiving field of view is considered to be equal to[2,4]

$$\Theta_{\text{com}} \cong \Theta_0 + 2\phi + 2L/R_{\min},$$

where ϕ is the angle between the optical axes of the emitting and the receiving systems, and subscript $_{\text{com}}$ means common system. Hence for $\phi = 0$ the minimal operating range of common wide-angle systems is approximately

$$R_{\min}^{\text{com}} = 2L/(\Theta_{\text{com}} - \Theta_0).$$

One can estimate numerically the increase of the stability against background radiation due to maintaining the optimal angular field of the receiver for $\phi = 0$ by considering a ratio of powers P_b of penetrating background flows in common and optimized cases:

$$U = P_b^{\text{com}}/P_b^{\text{opt}} = (\Theta_{\text{com}}/\Theta_{\text{opt}})^2$$
$$= [(\Theta_0 + 2L/R_{\min})/(\Theta_0 + d_0/R)]^2.$$

To estimate the SBR improving extent by calculating the lower limit of U, let us set $R = R_{\min}$ in the denominator of the last equation. Then

$$U_{\min} = (1 + 2L/R_{\min}\Theta_0)^2 = (1 + g)^2,$$

where g is the lidar system parameter, $g = 2L/\Theta_0 R_{\min}$, and we suppose that $R_{\min}\Theta_0 \gg d_0$ and $L \gg d_0$. For $g = 1 \ldots 10$ (for example, if $\Theta_0 \cong 1$ mrad, $L \cong 0.5$ m, $R_{\min} = 100 \ldots 1000$ m) the increasing SBR can reach values $V_t \cong 4 \ldots 121$. This means that a significant advantage in decreasing the background clutter can be obtained when the optimal field of view is used.

The authors intend to discuss technical means for optimization of field of view and to give detailed numerical estimations of reachable effects in a future article.

6. Practical Use of Wedgelike Field Diaphragm

The analysis carried out in the previous sections allowed the assessing of the fundamental limits of the background-radiation filtering. To do this the as-

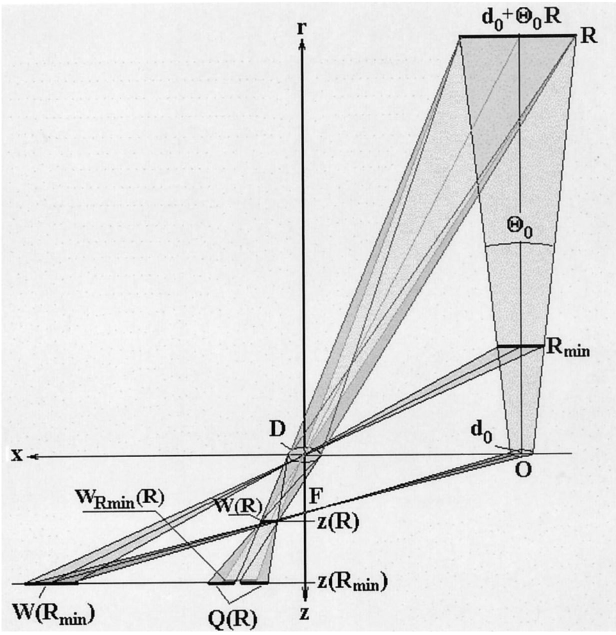

Fig. 4. Illustration of the R-layer image defocusing in the $R_{\min}$-layer image plane.

sumption that the background-filtering stop matched the profile of the scattering volume was implicit. As discussed in Section 4 this led to a wedge-shaped stop placed at an angle with respect to the focal plane.

While this ensures having the minimum field of view that accepts all return signals for all of the exploration range, it may be nonpractical from a mechanical standpoint. For mechanical simplicity one would in general prefer using a stop in a plane that is parallel to the focal plane at a distance $z(R_{\min})$ from it, given by the first of Eqs. (2). When the stop is parallel to the focal plane it cannot "follow" the image of the instantaneous scattering volume (whose position depends on the range, as discussed in Section 2), and defocusing effects must be taken into account, especially for the shorter ranges, if the total return signal is to be accepted. Such a situation is illustrated in Fig. 4.

If we assume the field stop is going to be placed on the $R_{\min}$-image plane (that lies at distance-$z(R_{\min})$ from the focus), we should take into account that the illumination law produced on the $z(R_{\min})$ plane by the signal echoed from a scattering volume at distance R will be the two-dimensional convolution of the illumination law produced in the $z(R)$ plane (that would in turn be a scaled version of the illumination law over the scattering volume) with a defocused spot formed from every point of the R-layer image by a lens of diameter D equal to the input-pupil diameter. Such a spot will be defocused up to the size (Fig. 4):

$$Q_{\text{spot}}^{R\min} = D(z_{R\min} - z_R)/(f + z_R) \cong fD(R - R_{\min})/R\, R_{\min}, \quad (7)$$

where $z(R)$ is given again by the first of Eqs. (2), and the approximation holds when $R \gg f$.

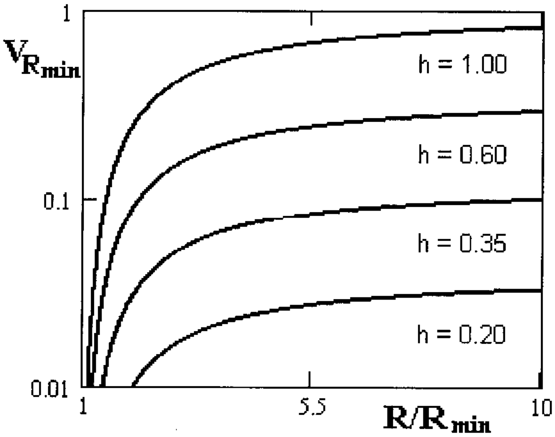

Fig. 5. Vignetting parameter $V_{R\min}$ as a function of $R/R_{\min}$ for different values of the system parameter h.

To evaluate the extent of the R-layer spot vignetting by the wedge-like diaphragm, and accepting the uniform distribution of the lidar signal intensity on the image cross section, we introduce a vignetting factor $V_{R\ \min}(\mathrm{R})$ as

$$V_{R\min}(R) = [Q_{\text{spot}}^{R\ \min}(R)/W_{R\min}(R)]^2. \quad (8)$$

Using Eqs. (3) and (8), assuming $R \gg f$, $\theta_0 \gg d_0/R_{\min}$, and introducing one more system parameter $h = D/\theta_0 R_{\min}$, we can obtain

$$V_{R\min}(R) \cong h^2(1 - R_{\min}/R)^2. \quad (9)$$

This expression is plotted as a function of $R/R_{\min}$ for several typical values of the parameter h in Fig. 5. According to it, for $h < 0.3$ we can consider the spot vignetting effect as small enough (<10%). Moreover, it is easy to check that if a Gaussian distribution of the radiation intensity on the image cross section is considered, the wedgelike diaphragm will give a better value of vignetting than for the uniform distribution.

7. Conclusions

The defined J figure of merit evaluates the spatial filtering efficiency of the lidar receiving system with regard to its ability to reject background radiation while accepting the backscattered laser signal. It allows us to compare different receiving-system designs from the point of view of their immunity against background radiation. To protect the optical system from background radiation one should devise a spatial filtering scheme leading to a J figure as close as possible to 1. In this case, however, ($J \approx 1$ that is illustrated in Fig. 2 by the case J_4) the traditional estimations of the signal–background ratio at the photodetector input that assume a field of view for background radiation equal to the instantaneous signal field of view are correct.

This work has been supported by the following contracts and grants: Government of Catalonia's Department of Universities, Research and Information

Society PIV 2000 program, project IMMPACTE of the Government of Catalonia's Interdepartment Commission for Research and Technological Innovation and Department of Environment, contract EVR1-CT-1999-40003 EARLINET of the European Commission, and grants REN2000-1754-C02-02 and REN2000-1907-CE of the Spanish Ministry for Science and Technology.

References

1. R. M. Measures, *Laser Remote Sensing: Fundamentals and Applications* (Wiley New York, 1984).
2. E. D. Hinkley, ed., *Laser Monitoring of Atmosphere* Vol. 14 of Topics in Applied Physics, (Springler-Verlag, Berlin, 1978).
3. R. R. Agishev, *Protection from Background Clutter in Electro-Optical Systems of Atmosphere Monitoring* (Mashinostroenie Press, Moscow, 1994), in Russian.
4. S. A. Danichkin and I. V. Samokhvalov, "Influence of optical system parameters on lidar characteristics," Sov. J. Opt. Technol. **46,** 5–8 (1979).
5. V. M. Orlov, I. V. Samokhvalov, and G. G. Matvienko, *Elements of Light Scattering Theory and Optical Radar* (Nauka Press, Novosibirsk, USSR, 1981), in Russian.
6. A. A. Tikhomirov, "Analysis of methods and technical means of dynamic range compression," Atmos. Oceanic Opt. **13,** 208–219 (2000).
7. V. E. Lystsev and V. G. Monastyrsky, "Some problems of scattering media photometry," in *Instruments and Methods of Remote Measurements of Atmospheric Optical Parameters* (Gidrometeoizdat Press, Leningrad, USSR, 1980), pp. 79–87, in Russian.
8. V. E. Zuev, B. V. Kaul, and I. V. Samokhvalov, *Laser Sensing of Industrial Aerosol* (Nauka Press, Novosibirsk, USSR, 1986), in Russian.